configuration self-consistent-field wave function.[16]

The failure of Koopmans' theorem for molecules with first-row transition-metal atoms is well documented.[14] It remains to be seen if this failure also includes the localization of the 3d hole in multinuclear compounds. This work presents the first direct experimental evidence, from the band shapes of the mixed-metal clusters, that this does occur. Although the concept of localization upon ionization provides a simple and unified explanation of several experimental and theoretical observations, it remains to be seen if this is the only explanation.

Acknowledgment. The authors thank the Robert A. Welch Foundation (Grant A-648) and the National Science Foundation (Grant CHE 79-20993) for support of this work.

Registry No. $SFeCo_2(CO)_9$, 22364-22-3; $SHFe_2Co(CO)_9$, 78547-58-7; $SH_2Fe_3(CO)_9$, 78547-62-3; $SH_2Ru_3(CO)_9$, 32574-35-9.

Department of Chemistry
Texas A&M University
College Station, Texas 77843

Peter T. Chesky
Michael B. Hall*

Received March 1, 1983

Articles

Contribution from the Division of Chemistry and Chemical Engineering, California Institute of Technology, Pasadena, California 91125, Applied Physics Laboratory, The Johns Hopkins University, Laurel, Maryland 20707, and Istituto di Chimica Fisica e Centro CNR, 20133 Milano, Italy

Polymorphism in Low-Dimensional Materials: X-ray Diffraction Studies on the Temperature Dependence of the Structure of α-Bis(1,2-benzoquinone dioximato)palladium(II)[1]

THOMAS J. KISTENMACHER* and RICCARDO DESTRO

Received July 14, 1982

X-ray diffraction studies on the structure of the α-form of bis(1,2-benzoquinone dioximato)palladium(II), α-$Pd(bqd)_2$, are reported. Detailed analyses of the structure at 295 and 122 K are presented. At 110 K a second-order phase transformation is observed and results in a commensurate supercell structure ($a' = a$, $b' = 4b$, $c' = c$) below the phase transition. Analysis of diffraction data collected at 76 and 19.5 K indicates that the superstructure results from both translation and rotation of the molecules and can be described in terms of a transverse modulation wave with a maximum displacement of 0.84 Å at 19.5 K. A model for the full supercell structure at 19.5 K has been developed and refined on the basis of superlattice intensity measurements.

Introduction

Structural phase transitions in quasi-one-dimensional inorganic and organic materials have been the subject of numerous physical, theoretical, and structural investigations.[2] As a phase transformation at a finite temperature reflects three-dimensional ordering, the evolution of a phase transition in these systems is sensitive to interchain coupling. In this respect, the phase transition in the prototypical inorganic compound $K_2Pt(CN)_4Br_{0.3}\cdot 3H_2O$ (KCP) is incomplete, with longitudinal and transverse correlation lengths of ~300 Å (about 100 Pt–Pt distances) and ~80 Å (about 9 interchain separations), respectively.[3] The absence of long-range transverse order in the longitudinally modulated low-temperture phase of KCP results from severe disorder in the charge-compensating halide anions and the solvent water molecules.[3]

The range of inorganic solids with quasi-unidimensional structural and electrical properties has been extended recently through the synthesis of the bis(1,2-dione dioximato)metal complexes of Ni(II), Pd(II), and Pt(II).[4] One interesting case arises with the complex $Pd(bqd)_2$ (Figure 1), where bqd is the chelating ligand 1,2-benzoquinone dioximate. Upon addition of a halogen such as I_2, this compound is partially oxidized to form a charge-transfer system[4f,i] with physical properties reminiscent of those displayed by KCP.[3]

The unoxidized $Pd(bqd)_2$ complex crystallizes in two polymorphic modifications at room temperature. In the α-form (orthohombic), the planar coordination complexes are stacked directly upon one another with their molecular planes rigorously perpendicular to the chain propagation direction.[5] In the β-form (monoclinic), the normals to the molecular planes

Table I. Crystallographic Data for α-$Pd(bqd)_2$ Prior to the Phase Transition

$Pd(C_6H_5N_2O_2)_2$, fw 380.63 $Z = 4$
orthorhombic, space group *Ibam* (D_{2h}^{26}) μ(Mo Kα) = 14.42 cm^{-1}

	295 (1) K	122 (1) K
a, Å	20.670 (3)	20.652 (3)
b, Å	9.737 (2)	9.709 (2)
c, Å	6.395 (1)	6.306 (1)
V, Å^3	1287.1	1264.4
density (X-ray), g cm^{-3}	1.964	2.000

* To whom correspondence should be addressed at the Applied Physics Laboratory, The Johns Hopkins University.

(1) Contribution No. 6406 from the Arthur Amos Noyes Laboratory of Chemical Physics, California Institute of Technology. Support of this research through the following granting agencies is gratefully acknowledged: (a) National Science Foundation, Grants DMR 74-19029A1 and DMR 78-23957; (b) National Institutes of Health, Grant GM 16966. R.D. also thanks the Fulbright-Hays Foundation for a travel grant.

(2) See, for example: Comes, R.; Shirane, G. In "Highly Conducting One-Dimensional Solids"; Devreese, J. T., Evrard, R. P., Van Doren, V. E., Eds.; Plenum Press: New York, 1979.

(3) (a) Comes, R.; Lambert, M.; Launois, H.; Zeller, H. R. *Phys. Rev. B* **1973**, *138*, 571. (b) Comes, R.; Lambert, M.; Zeller, H. R. *Phys. Status Solidi B* **1973**, *58*, 587. (c) Renker, B.; Rietschel, H.; Pintschovius, L.; Glaser, W.; Bruesch, P.; Kuse, D.; Rice, M. J. *Phys. Rev. Lett.* **1973**, *30*, 1144. (d) Renker, B.; Pintschovius, L.; Glaser, W.; Rietschel, R.; Comes, R.; Liebert, L.; Drexel, W. *Ibid.* **1974**, *32*, 836. (e) Lynn, J. W.; Iizumi, M.; Shirane, G.; Werner, S. A.; Saillant, R. B. *Phys. Rev. B: Solid State* **1975**, *12*, 1154. (f) Carneiro, K.; Shirane, G.; Werner, S. A.; Kaiser, S. *Ibid.* **1976**, *13*, 4258. (g) Eagen, C. F.; Werner, S. .; Saillant, R. B. *Ibid.* **1976**, *12*, 2036. (h) Williams, J. M.; Schultz, A. J.; Underhill, A. E.; Carneirs, K. In "Extended Linear Chain Compounds"; Miller, J. S., Ed.; Plenum Press: New York, 1981; Vol. 1.

0020-1669/83/1322-2104$01.50/0 © 1983 American Chemical Society

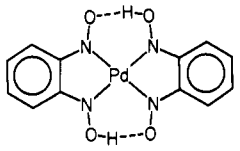

Figure 1. Molecular structure of bis(1,2-benzoquinone dioximato)-palladium(II), $Pd(bqd)_2$.

are inclined by about 25° to the stacking direction and the molecular overlap is between slipped molecular planes.[6] In the α-form, the presence of extended molecular chains, the moderate Pd–Pd separation (~3.2 Å), and overlapping of the frontier molecular orbitals[7] of the bqd ligands in the observed staggered orientation give rise to narrow electronic bands.[8] Similar bands are absent for the motif adopted by the β-modification. Evidence of the difference in the electronic structures for the two forms of $Pd(bqd)_2$ is shown by their optical reflectance spectra;[8] crystals of the α-form show optical anisotropies, characteristic of one-dimensional banding effects, while isotropic optical spectral bands are observed in the β-form. Similarly, Young's modulus and the internal friction for the α-polymorph show changes with temperature, while these effects are absent for the β-polymorph. Brill et al.[8] attributed the observed changes in Young's modulus and the internal friction for α-$Pd(bqd)_2$ to the presence of a phase transition that involves a displacement of the molecules.

As a means of clarifying the temperature dependence of the structural properties of the α-polymorph of $Pd(bqd)_2$ and, in particular, the nature of the phase transition, we have undertaken a single-crystal X-ray diffraction study of the temperature dependence of the crystal structure of this material. Previously,[9] we have briefly commented on the substructure–superstructure transformation in α-$Pd(bqd)_2$ near 110 K. Herein, we give detailed descriptions of the structure above the phase transition (at 295 and 122 K) and present a model for the low-temperature structure of α-$Pd(bqd)_2$ derived from X-ray diffraction data collected at 19.5 K.

Pretransition Studies

(a) Room-Temperature Diffraction Data and Analysis. The room-temperature crystal structure of α-$Pd(bqd)_2$ was originally reported by Leichert and Weiss.[5] However, peculiar values for the atomic thermal factors (notably for the components that describe the motion along the stacking direction) and the absence of hydrogen atom contributions suggested that a more accurate analysis was required for comparison with low-temperature results.

A suitable crystal was selected from a sample, supplied by Drs. J. W. Brill and M. Mêgnamisi-Bêlombê, and mounted on a locally modified Syntex $P2_1$ diffractometer. Unit-cell data at 295 K are presented in Table I; details of data collection and analysis are reported in Table II. The more conventional *Ibam* setting for space group D_{2h}^{26} was adopted, as opposed to the *Imcb* setting employed by Leichert and Weiss.[5] Difference-Fourier syntheses, computed during the course of the refinement, allowed the location of all hydrogen atoms (although the difference density in the region of the oxime proton was clearly elongated along the O···O vector of the O–H···O hydrogen-bond system; vide infra). Final positional parameters for all atoms are collected in Table III. The esd's reported

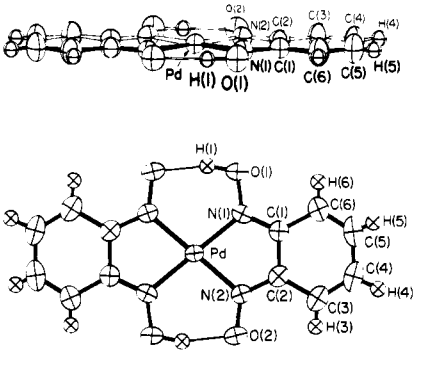

295 K

Figure 2. Two views of the molecular geometry and the molecular motion of the $Pd(bqd)_2$ complex in the α-$Pd(bqd)_2$ structure at 295 K.

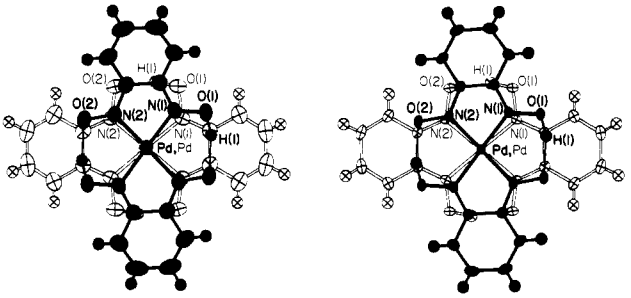

295 K 122 K

Figure 3. Intrachain molecular overlaps in the columnar arrays in the α-$Pd(bqd)_2$ structure at 295 and 122 K.

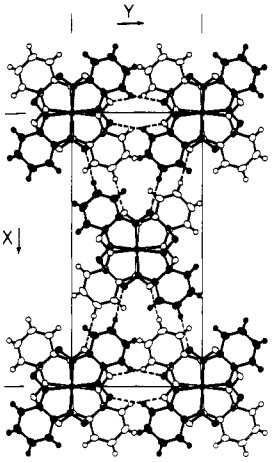

295 K

Figure 4. Crystal structure of α-$Pd(bqd)_2$ at 295 K. The dashed lines indicate the interchain C–H···O contacts; see the text and Table V.

(4) (a) Endres, H.; Keller, H. J.; Lehmann, R.; van de Sand, H.; Vu, D.; Poveda, A. *Ann. N.Y. Acad. Sci.* **1978**, *313*, 617. (b) Mêgnamisi-Bêlombê, M. *Ibid.* **1978**, *313*, 633. (c) Marks, T. J. *Ibid.* **1978**, *313*, 594. (d) Leichert, I.; Weiss, J. *Acta Crystallogr., Sect. B* **1975**, *B31*, 2709. (e) Endres, H.; Mêgnamisi-Bêlombê, M.; Little, W. A.; Wolfe, C. R. *Ibid.* **1979**, *35*, 169. (f) Endres, H.; Keller, H. J.; Mêgnamisi-Bêlombê, M.; Moroni, W.; Nothe, D. *Inorg. Nucl. Chem. Lett.* **1974**, *10*, 467. (g) Endres, H.; Keller, H. J.; Mêgnamisi-Bêlombê, M.; Moroni, W.; Pritzkow, H.; Weiss, J.; Comes, R. *Acta Crystallogr., Sect. A* **1976**, *A32*, 954. (h) Cowie, M.; Gleizes, A.; Grynkewich, G. W.; Kalina, D. W.; McClure, M. S.; Scaringe, R. P.; Teitelbaum, R. C.; Ruby, S. L.; Ibers, J. A.; Kannewulf, C. R.; Marks, T. J. *J. Am. Chem. Soc.* **1979**, *101*, 2921. (i) Brown, L. D.; Kalina, D. W.; McClure, M. S.; Schultz, S.; Ruby, S. L.; Ibers, J. A.; Kannewulf, C. R.; Marks, T. J. *Ibid.* **1979**, *101*, 2937.
(5) Leichert, I.; Weiss, J. *Acta Crystallogr., Sect. B* **1975**, *B31*, 2709.
(6) Endres, H.; Mêgnamisi-Bêlombê, M.; Little, W. A.; Wolfe, C. R. *Acta Crystallogr., Sect. B* **1979**, *B35*, 169.
(7) Miller, J. S. *Inorg. Chem.* **1977**, *16*, 957.
(8) Brill, J. W.; Mêgnamisi-Bêlombê, M.; Novotny, M. *J. Chem. Phys.* **1978**, *68*, 585.
(9) Kistenmacher, T. J.; Destro, R.; Marsh, R. E.; Samson, S. *Mol. Cryst. Liq. Cryst.* **1980**, *62*, 173.
(10) Wilson, A. J. C. *Nature (London)* **1942**, *150*, 151.
(11) (a) "International Tables for X-Ray Crystallography"; Ibers, J. A., Hamilton, W. C., Eds.; Kynoch Press: Birmingham, England, 1974; Vol. IV. (b) Stewart, R. F.; Davidson, E. R.; Simpson, W. T. *J. Chem. Phys.* **1965**, *42*, 3175.
(12) Cromer, D. T.; Waber, J. T. *Acta Crystallogr.* **1965**, *18*, 104.

Table II. Details of Pretransition Data Collection and Analysis

temp data collection, K	295 (1)	122 (1)
cryst dimens, mm		
(001)-(00$\bar{1}$)	0.267	0.333
(010)-(0$\bar{1}$0)	0.150	0.157
(100)-($\bar{1}$00)	0.050	0.053
technique of data collecn[a]		
scanning mode	θ-2θ	θ-2θ
scan rate, deg/min (in 2θ)	variable in the range 1.5–4	const at 1.5
max 2θ angle, deg	60	90
reflcns and averages[b]		
no. of reflcns measd	4578	6233
no. of sym-indep reflcns	1031	2794
no. of reflcns with net counts above bkgd ($I > 0$)	925	2423
assumed std dev (σ_c from counting statistics)	$\sigma = [\sigma_c^2 + (0.015I)^2]^{1/2}$	$\sigma = [\sigma_c^2 + (0.02I)^2]^{1/2}$
least-squares refinement[c]		
no. of reflcns in refinement (m)	1030[d]	2423
no. of refined parameters (n)	81	81
$R(F) = \Sigma \|\|F_o\| - \|F_c\|\|/\Sigma \|F_o\|$	0.034	0.061
$S = [\Sigma w(k^2F_o^2 - F_c^2)^2/(m-n)]^{1/2}$	2.13	1.53

[a] Mo Kα radiation, λ = 0.710 69 Å; graphite monochromator. No variations, other than those expected from counting statistics, were shown by three standard reflections frequently monitored during data collection. Background was measured at each side of scan for a time equal to one-fourth of the scan time. [b] Data were corrected for Lorentz and polarization effects; no absorption correction was deemed necessary. [c] The quantity minimized was $\Sigma w(|F_o^2| - |k'F_c^2|)^2$, with weights $w = 1/\sigma^2(F_o^2)$. Neutral-atom scattering factors for the non-hydrogen atoms were taken from compilations in ref 11a, while those for the H atoms were from the table of Stewart, Davidson, and Simpson.[11b] The real component of anomalous dispersion for Pd was accounted for by using the value given by Cromer and Waber.[12] [d] The weight of the reflection (200) was set equal to zero as the diffraction profile for this reflection was seriously affected by the diffracted beam stop.

in this table are 6–10 times smaller than those previously obtained,[5] as are the esd's for derived geometrical parameters, which are given in Table IV.

The $Pd(bqd)_2$ molecule has crystallographic $2/m$ (C_{2h}) symmetry. Views perpendicular to and approximately parallel to the molecular plane are shown in Figure 2. The mode of the molecular overlap within the one-dimensional chains along the c axis is shown in Figure 3. Miller[7] has rationalized this molecular overlap pattern on the basis of symmetry and molecular orbital overlap criteria. The basic format of the packing of columnar arrays in the room-temperature α-$Pd(bqd)_2$ motif is shown in Figure 4. The columnar arrays parallel c, with the shortest intermolecular contact between adjacent Pd atoms at 3.198 Å. The intercolumn binding forces appear to be of two types: (a) dispersive (van der Waals) forces between neutral complexes; (b) two unique C–H(quininoid)···O(oxime) interactions (providing direct coupling along the a and b axes) (Table V).

(b) 122 K Diffraction Data and Analysis. A locally designed and built diffractometer was used for data collection and has been described elsewhere.[13] The system maintains temperatures down to about 18 K for long periods of time with high precision (±0.5 K). Thus, we were able to ensure that any change in the intensity, position, or shape of a diffraction peak was complete.

From a knowledge[8] of the temperature dependence of Young's modulus for α-$Pd(bqd)_2$, it was decided that a temperature near 120 K would be suitably far above the phase transition but sufficiently below room temperature to allow us to study in detail the "normal" temperature dependence of the α-$Pd(bqd)_2$ structure. Thus, the crystal was slowly cooled (2–4 deg/h) to, and fully equilibrated at, 122 K.

Unit-cell dimensions at 122 K are reported in Table I. All three cell constants have contracted differently on reduction of the temperature. For the transverse a and b cell dimensions, significant contractions are observed (0.09% and 0.29%, respectively), while for c the contraction is much larger (1.39%) and reduces by 0.045 Å the Pd···Pd and molecular separations ($\Delta c/2$) and presumably strengthens the intermolecular coupling along the chain direction.

Table III. Atomic Positional Parameters at 295 and 122 K

atom (T, K)	x[a]	y
Pd (295)	0	0
(122)	0	0
N(1) (295)	1 126 (15)	20 217 (30)
(122)	1 086 (9)	20 256 (21)
N(2) (295)	9 541 (12)	1 073 (42)
(122)	9 591 (9)	1 001 (27)
O(1) (295)	−3 916 (13)	29 064 (31)
(122)	−3 928 (9)	29 177 (21)
O(2) (295)	13 334 (13)	−9 998 (32)
(122)	13 352 (9)	−10 066 (21)
C(1) (295)	7 121 (19)	24 501 (41)
(122)	7 121 (12)	24 586 (27)
C(2) (295)	11 884 (20)	13 693 (46)
(122)	11 980 (13)	13 692 (29)
C(3) (295)	18 636 (21)	17 320 (54)
(122)	18 687 (12)	17 300 (32)
C(4) (295)	20 300 (24)	30 615 (60)
(122)	20 410 (14)	30 717 (36)
C(5) (295)	15 473 (28)	41 218 (58)
(122)	15 603 (16)	41 452 (33)
C(6) (295)	9 223 (23)	38 522 (46)
(122)	9 224 (15)	38 692 (29)
H(1) (295)	790 (23)	2 363 (63)
(122)	−784 (22)	2 408 (60)
H(3) (295)	2 133 (21)	1 014 (43)
(122)	2 165 (18)	1 036 (36)
H(4) (295)	2 435 (17)	3 323 (37)
(122)	2 423 (15)	3 335 (32)
H(5) (295)	1 677 (17)	4 792 (42)
(122)	1 663 (15)	4 928 (35)
H(6) (295)	629 (16)	4 499 (34)
(122)	654 (15)	4 516 (32)

[a] The fractional coordinates of the non-hydrogen atoms have been multiplied by 10^5; the fractional coordinates of the hydrogen atoms have been multiplied by 10^4; the z coordinates are zero by symmetry.

Details of experimental procedures for data collection, data processing, and least-squares refinement are given in Table II; final positional parameters are listed in Table III. From room temperature to 122 K, there are only minor changes in the fractional coordinates (and consequently the derived molecular geometry, Table IV) with a maximum change/σ (295

(13) Samson, S.; Goldfish, E.; Dick, C. J. *J. Appl. Crystallogr.* **1980**, *13*, 425.

Table IV. Molecular Geometry at 295 and 122 K

	295 K	122 K
(a) Bond Lengths (Å) and Angles (deg) Involving the Non-Hydrogen Atoms		
Pd-N(1)	1.982 (3)	1.979 (2)
Pd-N(2)	1.975 (3)	1.983 (2)
N(1)-O(1)	1.352 (4)	1.350 (3)
N(2)-O(2)	1.333 (4)	1.326 (3)
N(1)-C(1)	1.308 (5)	1.315 (3)
N(2)-C(2)	1.321 (5)	1.327 (4)
C(1)-C(2)	1.441 (6)	1.458 (4)
C(1)-C(6)	1.433 (6)	1.437 (4)
C(2)-C(3)	1.440 (6)	1.429 (4)
C(5)-C(6)	1.318 (8)	1.344 (4)
C(3)-C(4)	1.340 (7)	1.350 (4)
C(4)-C(5)	1.436 (8)	1.439 (5)
O(1)···O(2)	2.690 (4)	2.689 (3)
N(1)-Pd-N(2)	80.2 (1)	80.69 (9)
N(1)-Pd-N(2′)	99.8 (1)	99.31 (9)
Pd-N(1)-O(1)	122.8 (2)	123.4 (1)
Pd-N(1)-C(1)	115.4 (3)	115.1 (2)
O(1)-N(1)-C(1)	121.8 (3)	121.5 (2)
Pd-N(2)-O(2)	123.0 (3)	123.0 (2)
Pd-N(2)-C(2)	114.5 (3)	114.6 (2)
O(2)-N(2)-C(2)	122.5 (3)	122.3 (2)
N(1)-C(1)-C(2)	114.5 (3)	114.9 (2)
N(1)-C(1)-C(6)	126.3 (3)	126.2 (2)
C(2)-C(1)-C(6)	119.3 (3)	118.9 (2)
N(2)-C(2)-C(1)	115.4 (3)	114.7 (2)
N(2)-C(2)-C(3)	125.7 (3)	126.0 (2)
C(3)-C(2)-C(1)	118.9 (3)	119.3 (2)
C(2)-C(3)-C(4)	119.1 (4)	119.5 (3)
C(3)-C(4)-C(5)	121.1 (5)	121.1 (3)
C(4)-C(5)-C(6)	122.5 (4)	122.1 (3)
C(1)-C(6)-C(5)	119.2 (5)	119.1 (3)
(b) Bond Lengths (Å) and Angles (deg) Involving the Hydrogen Atoms		
H(1)-O(1)	0.98 (7)	0.95 (5)
H(3)-C(3)	0.89 (6)	0.91 (4)
H(4)-C(4)	0.88 (5)	0.83 (3)
H(5)-C(5)	0.71 (5)	0.79 (3)
H(6)-C(6)	0.87 (5)	0.84 (3)
H(1)-O(1)-N(1)	108 (5)	109 (3)
C(2)-C(3)-H(3)	114 (5)	118 (2)
C(4)-C(3)-H(3)	127 (4)	123 (2)
C(3)-C(4)-H(4)	122 (4)	123 (2)
C(5)-C(4)-H(4)	117 (4)	116 (2)
C(4)-C(5)-H(5)	114 (4)	121 (2)
C(6)-C(5)-H(5)	124 (4)	117 (2)
C(1)-C(6)-H(6)	118 (4)	121 (2)
C(5)-C(6)-H(6)	122 (4)	120 (2)

[a] N(2′) is related to N(2) by the symmetry transform $-x, -y, z$.

K) of 4–5. There are considerably more relevant (and anisotropic) changes in the thermal factors. The average mean-squares displacements ($\bar{U}_{ii}$) are reduced by considerably different factors: the in-plane components $\bar{U}_{11}$ and $\bar{U}_{22}$ are reduced by 2.3 (1), while the component along the stacking axis, $\bar{U}_{33}$, is reduced by 2.0 (1) (numbers in parentheses are root-mean-square deviations of the ratios of the individual atom thermal factors from the average ratio). We note for comparison that the temperature ratio $T_{initial}/T_{final}$ (295 K/122 K) is 2.42. The implication is that the interchain forces—primarily the C–H···O interactions—are appreciably "softer" than the intrachain stacking forces.

Molecular illustrations derived from the 122 K structure analysis, analogous to those given in Figure 2 from the 295 K work, are shown in Figure 5. The significant reduction in the mean molecular motion at 122 K compared to room temperature is readily apparent from a comparison of Figures 2 and 5. On the average, the intramolecular bond lengths (Table IV) between non-hydrogen atoms have elongated by about

Table V. Principal Intra- and Intercolumn Interactions at 295 and 122 K

(a) Intracolumn Interactions (Å)

	295 K	122 K
Pd···Pd[a]	3.198 ($c/2$)	3.153 ($c/2$)
N(1)···N(1)[a]	3.231 (4)	3.185 (3)
N(1)···O(1)[a]	3.361 (4)	3.322 (3)
N(2)···N(2)[b]	3.204 (4)	3.159 (3)
N(2)···O(2)[b]	3.405 (4)	3.364 (3)
O(1)···C(1)[a]	3.295 (5)	3.252 (3)
O(2)···C(2)[b]	3.232 (5)	3.185 (3)
O(2)···C(3)[b]	3.454 (4)	3.413 (3)

(b) Intercolumn C–H···O Interactions

C	H	O	C···O, Å	H···O, Å	C–H···O, deg	temp, K
C(4)	H(4)	O(2)[c]	3.504 (5)	2.63 (5)	177 (4)	295
			3.471 (3)	2.64 (4)	177 (3)	122
C(6)	H(6)	O(1)[d]	3.341 (5)	2.57 (5)	147 (4)	295
			3.306 (3)	2.55 (4)	151 (3)	122

[a] $-x, y, 1/2-z$. [b] $x, -y, -1/2-z$. [c] $1/2-x, 1/2+y, -z$. [d] $-x, 1-y, z$.

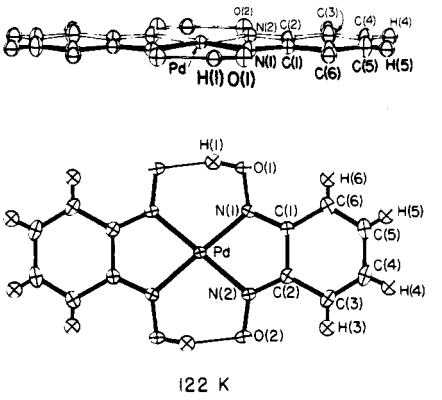

122 K

Figure 5. Two views of the molecular motion and the molecular geometry of the $Pd(bqd)_2$ molecule in the α-$Pd(bqd)_2$ structure at 122 K.

0.003 Å, but this elongation is by no means uniformly distributed over the molecular frame. Measurable elongations are noted in the C(1)–C(2) (0.017 Å) and the C(5)–C(6) (0.026 Å) bond lengths, both of which involve atoms near the terminus of the molecule. Similar small and sporadic differences are also seen in the intramolecular bond angles. The only noteworthy ones are the opening of the chelate bite angle [N(1)–Pd–N(2)] by 0.4° and a concurrent closing of the N(1)–Pd–N(2′) bond angle by the same amount.

The changes in the intermolecular contacts from 295 to 122 K are considerably larger than the intramolecular changes. Besides the contraction by 0.045 Å between molecular planes along the stacking axis, there is a reduction by 0.04 Å in the already short C–H···O[C(6)–H(6)···O(1)] interstack contact and a slightly smaller contraction, by 0.03 Å, in the longer C–H···O interstack contact (Table V). There is, however, no basic change in the mode of the intrastack overlap pattern (Figure 3) nor the structural motif (Figure 4) down to 122 K.

Finally, we devote a brief discussion to the intramolecular O–H···O hydrogen-bond system. Positions for all the hydrogen atoms have been obtained at 295 K and, more convincingly, at 122 K. The intramolecular O(1)···O(2) separation is large and essentially temperature independent [2.690 (7) Å (295 K) and 2.686 (5) Å (122 K)]. It has been established in a variety of similar molecular systems that the O–H···O hydrogen bond should be asymmetric for O···O separations over ~2.4–2.5 Å.[14] An asymmetric intracomplex hydrogen bond

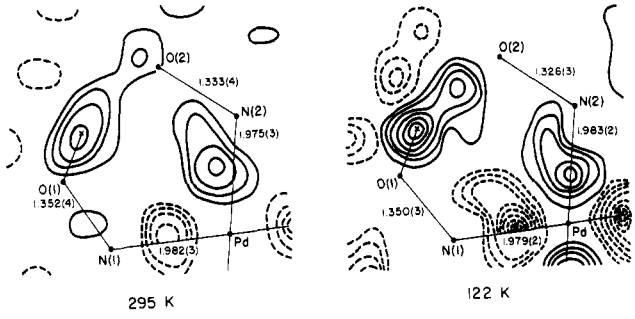

Figure 6. Final difference-density syntheses (295 and 122 K) in the region of the oxime hydrogen atom. The oxime hydrogen atom did not contribute to the calculated structure factors. The contours start at ±0.1 e/Å^3 (positive contours as solid lines, negative contours as dashed lines), with increments or decrements of 0.1 e/Å^3.

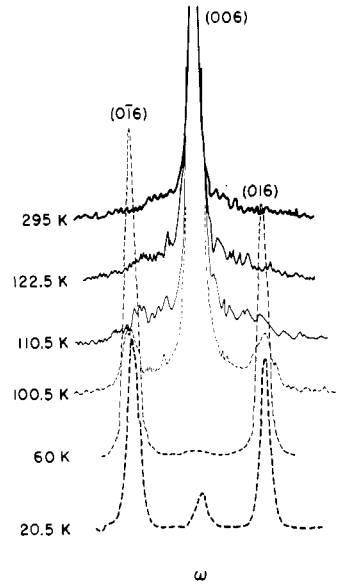

Figure 7. Temperature dependence of one sublattice, (006), and two superlattice, (016) and (0$\bar{1}$6), reflections.

has, in fact, been experimentally verified at both 295 and 122 K; see Figure 6. However, there is clear indication that the oxime proton H(1) is distributed over two sites—one near oxygen atom O(1) and one near oxygen atom O(2). At 122 K, the site occupancies are approximately 60% and 40% as judged from the peak heights on the difference map, Figure 6.

Diffraction Indicators of the Phase Transition

The diffraction profiles of several reflections were monitored while reducing the crystal temperature at a rate of 2–4 deg/h. For the pinacoid reflections (006), (040), and (400), abrupt narrowing of the peak profiles at ~110 K is observed near the same temperature at which there is a change in the slope of Young's modulus.[8]

Accompanying the peak narrowing at ~110 K is the appearance of superlattice reflections. These reflections can be indexed in a primitive, commensurate[15] supercell, which has a volume 4 times that of the body-centered high-temperature cell ($a' = a$, $b' = 4b$, $c' = c$).[9] We associate the *change in space group* observed near 110 K with the *transition temperature*.[16] This is in contrast to the Young's modulus data from which Brill et al.[8] deduced a transition temperature of ~90 K, where

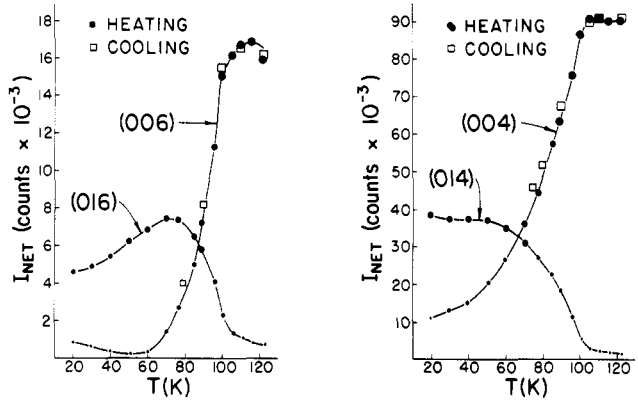

Figure 8. Temperature dependence of the net intensities of two sublattice, (006) and (004), and two superlattice, (016) and (014), reflections. Both heating and cooling data are presented. Solid lines are meant as a "guide to the eye". The relative size of each datum point is bounded at 1 esd.

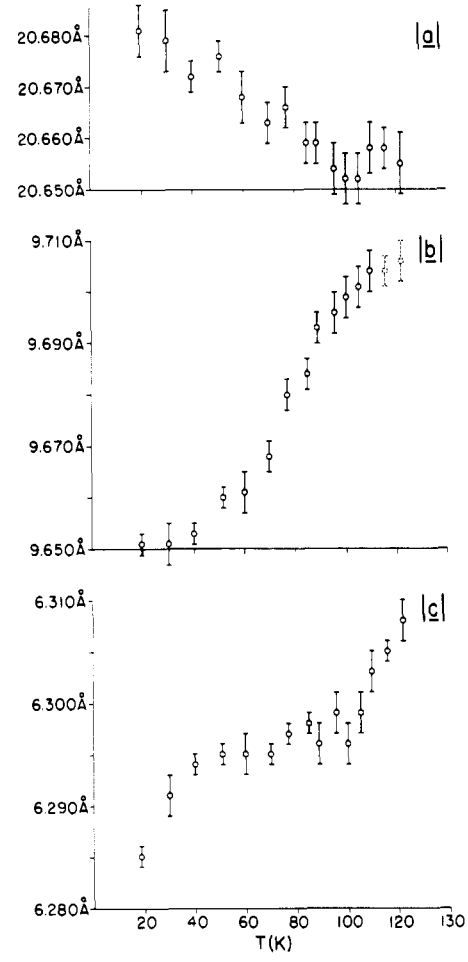

Figure 9. Variation with temperature for the unit-cell constants of α-Pd(bqd)$_2$. For $T > T_0$, the b cell constant is about 9.7 Å (dashed circles); below T_0, b quadruples and superlattice reflections (h,k/4,l) in the subcell indexing) are observed. Error bars indicate 1 esd.

the internal friction is a maximum and the inflection point in Young's modulus is reached.

In Figure 7, ω-scans for the subcell reflection (006) and its two first-order satellites (016) and (0$\bar{1}$6) as a function of temperature are shown. Recycling through the phase transition (Figure 8) shows no indication of hysteresis in the diffraction intensity variation, in accord with the absence of hysteresis in the Young's modulus data of Brill et al.[8]

In addition, the changes in the unit-cell dimensions have been monitored from above (122 K) to below (20 K) the phase

(14) See, for example: Marzilli, L. G.; Epps, L. A.; Sorrell, T.; Kistenmacher, T. J. *J. Am. Chem. Soc.* **1975**, *97*, 3351.
(15) Cowley, J. M., Cohen, J. B., Salamon, M. B., Wuensch, S., Eds. *AIP Conf. Proc.* **1979**, *No. 53*.
(16) Landau, L. D.; Lifshitz, E. M. In "Statistical Physics"; Pergamon Press: New York, 1958; Vol. 5, pp 430–456.

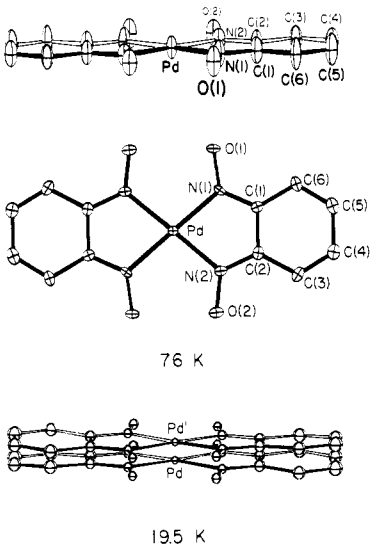

Figure 10. Results of the subcell refinements at 76 and 19.5 K.

transition (Figure 9). For the transverse cell constant a, a change in slope at the phase transition is noted, but somewhat surprisingly a elongates on cooling to about 40 K where there is indication of saturation. Except for the quadrupling noted at the onset of the phase transition, the other transverse cell constant b shows contraction with temperature and evidence of saturation at ~40 K. The longitudinal cell constant c exhibits several interesting features (Figure 9). There is a contraction with decreasing temperature above the phase transition. At the phase transition, dc/dT abruptly changes and then remains constant until about 40 K but, in contrast to the transverse cell constants, shows *no* evidence of saturation at low temperature. In fact, dc/dT below 40 K appears to revert to the same value as above the phase transition. The variation of c with temperature is similar to that of Young's modulus,[8] with the exception that, while c is temperature independent between 100 and 40 K, Young's modulus is not.

Posttransition Studies

(a) Subcell Refinements at 76 and 19.5 K. In an attempt to deduce the nature of the supercell structure, the *average* subcell structure (based on space group *Ibam*) at 76 and 19.5 K was studied. At 76 K, subcell constants are a = 20.659 (3) Å, b = 9.684 (3) Å, and c = 6.292 (1) Å. These parameters can be compared to those obtained at 295 and 122 K as given in Table I. A set of subcell data (the hkl octant to $2\theta = 60°$) were collected on the low-temperature diffractometer. A total of 1011 independent reflections (915 positive) were collected and analyzed.

As a starting point for the 76 K subcell refinement, the 122 K refined model was used, with the exclusion of the contributions of the hydrogen atoms. Four cycles of refinement quickly led to convergence and to final R and goodness-of-fit values of 0.049 and 2.16, respectively. The same molecular illustrations as presented at 295 K (Figure 2) and 122 K (Figure 5) are given for the 76 K model in Figure 10. It is evident on comparing these three figures that the apparent thermal motion normal to the molecular plane and paralleling the stacking direction is extended in the 76 K refinement. Quantitatively, the transverse thermal components $\bar{U}_{11}$(76 K) and $\bar{U}_{22}$(76 K) are about 70% of those at 122 K, while the $\bar{U}_{33}$ component is approximately 250% *larger* than at 122 K.

A similar substructure refinement was also performed on data measured at the lowest attainable temperature (19.5 K). Here, a complete set of both subcell and supercell data was collected (to $2\theta = 40°$), by using the moving-crystal, stationary-counter ω-scan technique. Cell constants for the 19.5 K supercell are collected in Table VI. The 3350 surveyed

Table VI. Crystallographic Data for α-Bis(1,2-benzoquinone dioximato)palladium(II) at 19.5 K

$a' = a = 20.679$ (10) Å	$V' = 4V = 5016.5$ Å^3
$b' = 4b = 38.592$ (16) Å	$((\sin\theta)/\lambda)_{max} = 0.48$ Å^{-1}
$c' = c = 6.286$ (2) Å	space group: $Pcc2$ (C_{2v}^3) or $Pca2_1$ (C_{2v}^5)
$Z = 16$	

reflections were corrected for Lorentz, polarization, and background effects.[17] After averaging of multiple measurements, the final superlattice data set (in space group $Pcc2$) consisted of 2625 independent reflections, of which 815 had $I < 0$ and were given zero weight. For the set with $I > 0$, weights were assigned as before. The number of reflections measured twice or more was 439, and the R value on averaging was 1.8%.

From these superlattice data, a set of subcell reflections ($k/4$ integral) were collated and yielded 331 total subcell reflections of which 309 were positive. Anisotropic refinement was initiated with the parameters from the 76 K subcell refinement. Four cycles of refinement were performed and gave R = 0.045 and a goodness-of-fit of 2.77. However, several aspects of this analysis were physically unreasonable. In particular, the U_{22} thermal components for atoms N(1) and O(2) were negative, and all U_{33} components were very large. A model was then tried in which the complex was offset from the crystallographic mirror plane paralleling (001) by the average root-mean-square displacement along c. In this "split" model, isotropic thermal parameters for all atoms were employed. Four cycles of refinement led to convergence with R = 0.052 and a goodness-of-fit of 2.97. A view approximately parallel to the mean molecular frame of the split model is presented in Figure 10.

Two very important pieces of information were derived from the subcell refinements at 76 and 19.5 K. First, there is a discernible modulation of the subcell structure to obtain the supercell structure, and the modulation vector is along c and increases in magnitude on going from 76 to 19.5 K. Second, the displacements of individual atoms of the $Pd(bqd)_2$ complex from the crystallographic mirror plane in the 19.5 K "split" model are not uniform (Figure 10), suggesting that there are molecular rotations as well as molecular translations on going from the substructure to the superstructure.

(b) Space Group and Derivation of the 19.5 K Supercell. The superlattice reflections that appear at the onset of the phase transition are inconsistent with retention of a body-centered space group as found above the phase transition. Also the $h0l$ reciprocal-lattice net is insensitive to the phase transition and, therefore, devoid of superlattice reflections. This net then possesses the same conditions limiting possible reflections, namely $h = 2n$ ($l = 2n$), as above the phase transition. These conditions can now be considered as arising from any of three possible glide operations (a, c, or n) parallel to the (010) crystallographic plane. Thus, some ambiguity is present in the space group determination. Careful scrutiny of the remaining principal reciprocal-lattice nets and line suggested that either of two space groups, $Pca2_1$ (C_{2v}^5) and $Pcc2$ (C_{2v}^3), could describe the systematics of the superlattice diffraction pattern. Both of these space groups (1) are noncentrosymmetric, (2) are *polar*, with the polar axis parallel to the columnar chain direction, and (3) are *subgroups* of the high-temperature space group *Ibam* (D_{2h}^{26}).

A three-dimensional Patterson synthesis based on the full superlattice data indicated that there were Pd atoms at various

(17) The quality of the data at 19.5 K was checked by careful analysis of the diffraction profiles and background measurements for each of the 3350 reciprocal lattice points. In only a very few cases (78 reflections with $I_{net} > 0$ and ca. 100 reflections with $I_{net} < 0$) were the background measurements in contrast with the profile behavior. In these cases, the total background was estimated on the basis of the average values of the last steps of each extremum of the profile.

Table VII. Translational[a] and Rotational[b] Displacements Applied to the 122 K Subcell Model To Yield the 19.5 K Supercell Model

molecule	Δx	Δy	Δz	θ_a, deg	θ_c, deg
A	0.0000	0.0000	0.0000[c]	0.0	0.0
B	−0.0027	0.2521	0.0676	−7.0[d]	0.0
C	0.0000	0.5000	0.1331	0.0	0.0
D	0.4990	0.1263	0.0189	−3.0	−1.0
E	0.5003	0.3759	0.1156	−4.0	0.0

[a] Δx, Δy, and Δz are fractional coordinate shifts (in terms of the 19.5 K cell) applied to the full origin-centered molecule of the 122 K refined model. [b] θ_a and θ_c are the rotations about the crystallographic a and c axes needed to extend the 122 K subcell model to the 19.5 K supercell model. When more than one rotation is necessary (molecule D), the rotation about c is applied first and followed by the rotation about a. [c] The z coordinate of molecule A has been arbitrarily set to 0.0 to define the origin along c in the polar space group $Pcc2$. [d] Negative rotations are counterclockwise about the positive crystallographic axis.

heights along the c axis. A careful study of the Patterson vectors in conjunction with packing arguments and difference-Fourier syntheses allowed the development of two supercell models, one in space group $Pcc2$ and one in $Pca2_1$, both of which gave R values of ~25%. These two models, while presented in different space groups, describe the same basic supercell structure. Functionally, it was decided that $Pcc2$ would be a better choice, since the twofold axis could be incorporated in the symmetry of some of the molecules.

Refinement of the supercell model proceeded by difference-Fourier methods and required, for some molecules, rotations about the crystallographic a and c axes as well as translations of the centers of mass. Proceeding in this fashion and assuming an isotropic thermal parameter of 1.2 Å^2 for all 125 atoms of the asymmetric unit (including hydrogen atoms) yielded an R value of 0.09 for the 973 reflections (319 sublattice and 654 superlattice) with $F_o^2 > \sigma(F_o^2)$. A subsequent difference-Fourier synthesis showed positive residues at the Pd atom positions; one residue was particularly noteworthy at ~4.3 e/Å^3. A further structure factor calculation using B = 1.0 Å^2 for the Pd atoms and retaining B = 1.2 Å^2 for the remaining atoms gave R = 0.08 for the 973 reflections with $F_o^2 > \sigma(F_o^2)$ and 0.12 for the 1810 reflections with $F_o^2 > 0$. A subsequent difference-Fourier synthesis showed a maximum residual density peak of 2.4 e/Å^3 at any Pd atom. The molecular translations and rotations that describe the supercell model are given in Table VII.

(c) Description of the Supercell Model. In Figure 11 are shown two principal crystallographic projections, (001) and (100), for the 19.5 K supercell model in the polar space group $Pcc2$. Of the five independent $Pd(bqd)_2$ molecules necessary to fully describe the low-temperature phase, two (labeled A and C in Figure 11) have imposed crystallographic symmetry 2 (C_2), while the remaining three (labeled B, D, and E) lie in general positions.

In descriptive terms, the supercell structure is a transverse modulation of the high-temperature subcell structure brought about by displacement of adjacent stacks along the chain-propagation axis c and by rotation of $Pd(bqd)_2$ molecules within each stack by up to 7° (Table VII). The result is an undulation of molecular stacks that can be described as a transverse packing wave with period $b' = 4b$ and amplitude 0.42 Å, as is most easily seen in the (100) projection (bottom of Figure 11). Our data do not demand nor does our model include any perturbations of the uniform stack motif along the chains of $Pd(bqd)_2$ molecules other than the slight modifications in the overlap of nearest neighbors indicated by the small molecular rotations of Table VII.

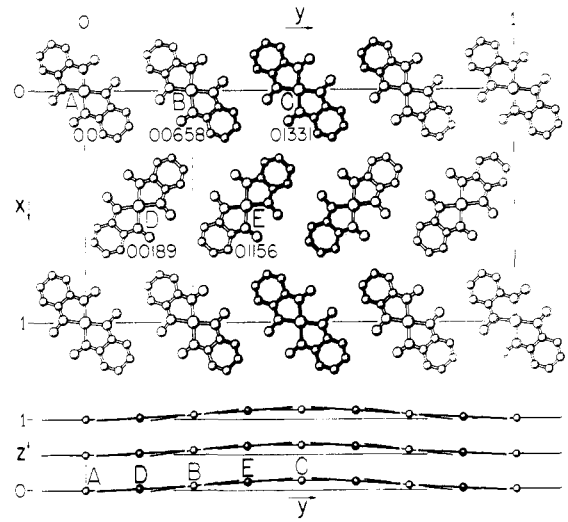

Figure 11. The superstructure at 19.5 K for α-$Pd(bqd)_2$. Top: one layer of molecules viewed along the stacking direction c. The relative heights of the five independent molecules are given in fractions of c (=6.28 Å); the dashed lines demarcate the 295 K subcell, in which all molecules are at a height of 0.0. Bottom: view along a, showing the modulated packing wave along b.

The relative displacements of adjacent stacks along c require only the modification of the weak C–H···O contacts and small alterations in the interchain dispersive forces. In light of the rather dramatic strengthening of the intrachain coupling with decreasing temperature (vide supra), the preference for the relaxing of interchain rather than intrachain coupling at low temperature is perhaps to be expected.

Summary

Detailed observations have been made by X-ray diffraction methods on the temperature dependence of the structure of the α-polymorph of the molecular complex $Pd(bqd)_2$. Down to about 110 K, the structure exhibits a normal temperature dependence, with a significant tightening of the cohesive forces (nominally banding in character) along the one-dimensional stacks of $Pd(bqd)_2$ molecules and to a lesser extent tightening of the essentially dispersive interchain forces. Near 110 K, a structural phase transition (consistent with Young's modulus data[8]) occurs, which is displacive in nature and leads to a transversely modulated ($b' = 4b$) packing motif.

Acknowledgment. The authors thank Drs. Richard E. Marsh, Sten O. Samson, William P. Schaefer, and Harry B. Gray and the Division of Chemistry and Chemical Engineering at California Institute of Technology for their hospitality during the 1978–1979 academic year, when the experimental work reported here was performed.

Registry No. α-$Pd(bqd)_2$, 53231-32-6.

Supplementary Material Available: Tables of atomic parameters and observed and calculated structure factor amplitudes for the subcell data sets at room temperature and 122 K and the supercell data set at 19.5 K (61 pages). Ordering information is given on any current masthead page.